Experimental Neurology 317 (2019) 119–128

Contents lists available at ScienceDirect

Experimental Neurology

journal homepage: www.elsevier.com/locate/yexnr

Research Paper

# Self-propagating, non-synaptic epileptiform activity recruits neurons by endogenous electric fields

Rajat S. Shivacharan[1], Chia-Chu Chiang[1], Mingming Zhang, Luis E. Gonzalez-Reyes, Dominique M. Durand*

*Department of Biomedical Engineering, Case Western Reserve University, Cleveland, OH 44106, USA*

ARTICLE INFO

*Keywords:*
Ephaptic coupling
Electric fields
Hippocampus
Epilepsy
Non-synaptic propagation

ABSTRACT

It is well documented that synapses play a significant role in the transmission of information between neurons. However, in the absence of synaptic transmission, neural activity has been observed to continue to propagate. Previous studies have shown that propagation of epileptiform activity takes place in the absence of synaptic transmission and gap junctions and is outside the range of ionic diffusion and axonal conduction. Computer simulations indicate that electric field coupling could be responsible for the propagation of neural activity under pathological conditions such as epilepsy. Electric fields can modulate neuronal membrane voltage, but there is no experimental evidence suggesting that electric field coupling can mediate self-regenerating propagation of neural activity. Here we examine the role of electric field coupling by eliminating all forms of neural communications except electric field coupling with a cut through the neural tissue. We show that 4-AP induced activity generates an electric field capable of recruiting neurons on the distal side of the cut. Experiments also show that applied electric fields with amplitudes similar to endogenous values can induce propagating waves. Finally, we show that canceling the electrical field at a given point can block spontaneous propagation. The results from these *in vitro* electrophysiology experiments suggest that electric field coupling is a critical mechanism for non-synaptic neural propagation and therefore could contribute to the propagation of epileptic activity in the brain.

## 1. Introduction

The hippocampus is a common focus of seizures or epileptiform activity in mesial temporal lobe epilepsy and important for basic neural functions such as memory consolidation or spatial navigation (Maguire et al., 2000; Jeffery et al., 2004; Morris et al., 1982). The hippocampal neural circuitry is organized into lamellae, or parallel strips of tissue in the transverse plane connected along the longitudinal direction (Amaral and Witter, 1989). Although it has been reported that there are synaptic connections both in the transverse and longitudinal directions (Ishizuka et al., 1990; Gloveli et al., 2005; Yang et al., 2014), recent observations show that spontaneous activity can propagate in hippocampus at speed much slower that synaptic/axonal conduction. Neural signals, especially epileptiform activity, can propagate along both the transverse and longitudinal septal-temporal axis of the hippocampus at speeds ~0.1 m/s in both *in-vitro* models and human patients (Gloveli et al., 2005; Zhang et al., 2014; Schevon et al., 2012). Spontaneous epileptiform activity generated by 4-Aminopyridine (4-AP) in the CA3 region travels longitudinally at a speed of 0.09 ± 0.03 m/s (Kibler and Durand, 2011). In the presence of picrotoxin, activity propagates longitudinally at 0.14 ± 0.04 m/s (Miles et al., 1988). Epileptiform behavior induced by high $K^+$ aCSF, low $Mg^{2+}$ aCSF, and non-synaptic low $Ca^{2+}$ aCSF generates activity propagating at 0.07 to 0.15 m/s (Liu et al., 2013; Quilichini et al., 2002; Haas and Jefferys, 1984). Under physiological conditions, slow periodic activity or slow wave sleep propagates in the hippocampus and the neocortex with a mean speed around 0.1 m/s (Chiang et al., 2019; Sanchez-Vives and McCormick, 2000). Therefore, 0.1 m/s is a common propagating speed, and as a result, a non-synaptic fundamental propagation mechanism may underlie many of these events.

Several studies suggest that epileptiform activity can propagate by non-synaptic mechanisms (Fröhlich and McCormick, 2010; Dudek et al., 1998). It has been shown that spontaneous epileptiform activity can still travel at ~0.1 m/s in the presence of presynaptic-blockers such as low $Ca^{2+}$ aCSF and gap junction blockers such as mefloquine (Zhang et al., 2014). Other propagation mechanisms (ionic diffusion and

* Corresponding author at: Departments of Biomedical Engineering, Neurosciences, and Physiology & Biophysics, Case Western Reserve University, 10900 Euclid Ave, Wickenden Bldg. Rm. 112, Cleveland, OH 44106, USA.
*E-mail address:* Dominique.Durand@case.edu (D.M. Durand).
[1] These authors have equal contribution.

https://doi.org/10.1016/j.expneurol.2019.02.005
Received 26 September 2018; Received in revised form 18 January 2019; Accepted 8 February 2019
Available online 15 February 2019
0014-4886/ 

axonal conduction) have very different propagation speeds. Seizure-like activity caused by the diffusion of $K^+$ ions propagate at speeds from 0.0004 to 0.008 m/s (Lian et al., 2001; Weissinger et al., 2000; Durand et al., 2010a). Axonal conduction velocity in the hippocampus varies from 0.3 to 0.5 m/s (Kibler and Durand, 2011; Miles et al., 1988; Jensen, 2008; Meeks and Mennerick, 2007). Therefore, the observed epileptiform activity propagating at approximately 0.1 m/s is independent of all the above-mentioned mechanisms. Therefore, electric field coupling, or ephaptic coupling, is the only other mechanism of communication between neurons that could explain these results.

Electric field coupling has been observed in cortical neurons, but it is thought to be too weak to mediate self-propagating activity (Anastassiou et al., 2011). Extracellular voltages can be modulated by weak electrical fields around the soma and dendrites, and externally applied electric fields can affect pharmacologically evoked hippocampal network activity (Fröhlich and McCormick, 2010; Francis et al., 2003; Jefferys, 1981; Terzuolo and Bullock, 1956). Electric fields have also been shown to synchronize neurons and axons, allowing for specific action potential timing with relatively constant propagation speeds (Bokil et al., in press; Radman et al., 2007). Recently published studies by our group have provided empirical and theoretical evidence that endogenous electric fields could underlie non-synaptic propagation under both pathological (Zhang et al., 2014; Qiu et al., 2015; Chiang et al., 2018) and physiological conditions (Chiang et al., 2019). Furthermore, it has been shown experimentally that 4-AP induced non-synaptic epileptiform waves are NMDA-dependent and computer simulations support the hypothesis that propagation of NMDA-dependent waves can only propagate by electric field coupling (Chiang et al., 2018). Computer simulation experiments suggest that electric field coupling could explain the non-synaptic epileptiform propagation, and predict that osmolarity changes should affect the speed. *In vitro* experiments confirmed that changing the osmolarity (*i.e.*, increasing and decreasing the extracellular space) results in a corresponding decrease or increase in speed (Qiu et al., 2015).

Taken together, these observations suggest that NMDA-sensitive extracellular waves induced by 4-AP are self-propagating by electric field coupling. Therefore, the purpose of this study is to determine if electric field coupling is both a necessary and sufficient mechanism to explain the propagation of spontaneous epileptiform activity.

## 2. Materials & methods

### 2.1. Longitudinal hippocampal slice preparation

Experimental protocols were reviewed and approved by the Institutional Animal Care and Use Committee (IACUC) at Case Western Reserve University. CD1 mice from Charles River or VSFP-Butterfly 1.2 transgenic mice (for imaging) from The Jackson Laboratory of either sex aged P10-P20 were anesthetized using isoflurane. Upon decapitation, the brain was placed in an ice cold (3–4 °C), oxygenated (95% $O_2$, 5% $CO_2$), sucrose enriched artificial cerebral spinal fluid (aCSF) solution. The brain was then sectioned by removing the cerebellum and separating the two hemispheres along the midline. From each hemisphere, the hippocampus was extracted from the temporal lobe of the brain (Fig. 1A). Longitudinal slices were made by placing the extracted hippocampi on a-custom made agar gel block, with the hippocampal sulcus facing up, and rotated by 90°. The rotated hippocampus-gel was then glued to the stage of the vibratome (VT1000S, Leica Microsystems). Another agar gel block was placed on the other side of the hippocampus to stabilize the tissue while slicing. The tissue was sliced in an oxygenated sucrose bath to a thickness of 400 μm and then transferred to a chamber contained oxygenated aCSF. Slices were incubated for at least one-hour post-surgery at room temperature (25 °C) prior to recording.

### 2.2. Solution preparation to elicit spontaneous epileptiform activity

Normal aCSF buffer solution consists of the following (in mM): 124 NaCl, 3.75 KCl, 1.25 $KH_2PO_4$, 2 $MgSO_4$, 26 $NaHCO_3$, 10 Dextrose, and 2 $CaCl_2$. Sucrose enriched aCSF buffer solution contains (in mM): 220 Sucrose, 2.95 KCl, 1.3 $NaH_2PO_4$, 2 $MgSO_4$, 26 $NaHCO_3$, 10 Dextrose, 2 $CaCl_2$. To elicit a spontaneous epileptiform activity from the tissue, 100 μM 4-aminopyridine (4-AP), a Kv1 potassium channel blocker was added to normal aCSF. Low $Ca^{2+}$ aCSF, commonly used to block synaptic transmission by inhibiting pre-synaptic neurotransmitter release, was made with the following recipe (in mM): 124 NaCl, 5.25 KCl, 1.25 $KH_2PO_4$, 1.5 $MgSO_4$, 26 $NaHCO_3$, 10 Dextrose, and 0.2 $CaCl_2$.

### 2.3. Electrophysiology recording setup

An interface perfusion slice chamber (BSC-ZT, Harvard Apparatus) that keeps tissue viable with temperature control and oxygenation was used to conduct the experiments in this study. The longitudinal slice was transferred from the recovery chamber to the interface chamber that has oxygenated and temperature controlled (32–34 °C) normal aCSF solution perfusing over the tissue slice. Glass recording electrodes were made from pulled fire-polished borosilicate glass micropipettes (0.5 mm inner diameter, 1.0 mm outer diameter) filled with 150 mM NaCl solution. An Ag/AgCl wire connected the filled glass recording electrode to an HS-2A head stage with a gain of one (Molecular Devices). The reference electrode for the recording electrodes was placed parallel to the tissue slice in the aCSF solution environment. All signals were amplified using an Axoclamp-2A microelectrode amplifier (Axon Instruments), and low-pass filtered (5 kHz field potentials) with additional amplification (FLA-01, Cygnus Technology). The signal is then digitized at 40 kHz by a recording data acquisition unit (PowerLab, AD Instruments), and stored in a computer for further analysis. The direction of spontaneous propagation is determined in real time during experimental recording for use in each study.

### 2.4. Optical recording setup

The optical recording setup for the imaging data presented here has been described in a previous study (Chiang et al., 2018). To summarize, to optically record from the VSFP-Butterfly 1.2 transgenic mice, a filter set was used to target mCitrine. The recording optics include the following filters and splitter: FF01-483/32-25 for mCitrine excitation (Semorck), FF01-542/27 for mCitrine emission (Semorck), and 515LP as the beam splitter for mCitrine. A broad-spectrum LED light source (X-cite 120LED, Excelitas Technologies) was used during the experiment. For the calcium imaging experiments, the excitation filter was 488 nm, the emission filter was 520 nm, and the dichroic mirror had a separation wavelength of 516 nm (Semrock, USA). Optical images were acquired using a digital CMOS camera (C11440, Hamamatsu Photonics) at a frame rate of 800 Hz (512 × 64 pixels, 4 × 4 binning). The imaging data was analyzed with MATLAB and a signal process toolbox (Math Works). All the acquired image sequences were filtered using 4 × 4 spatial filters to eliminate electron noise from the camera and shot noise from the acquisition electronics. The fluorescent signals were presented as a percentage of fluorescent change, $\Delta F/F_0$, which was calculated as $(F-F_0)/F_0$, where $F_0$ is the baseline fluorescence signal.

### 2.5. Extracellular electric field clamp

We have developed and tested a novel experimental system capable of clamping the extracellular electric field to zero locally, thereby preventing a neural signal from propagating by electric fields only. This device is based on the voltage clamp system commonly used for intracellular work but modified for extracellular fields. The circuit was validated and tested through computer modeling and benchtop testing under the aCSF solution (See supplementary Fig. S2). The benchtop

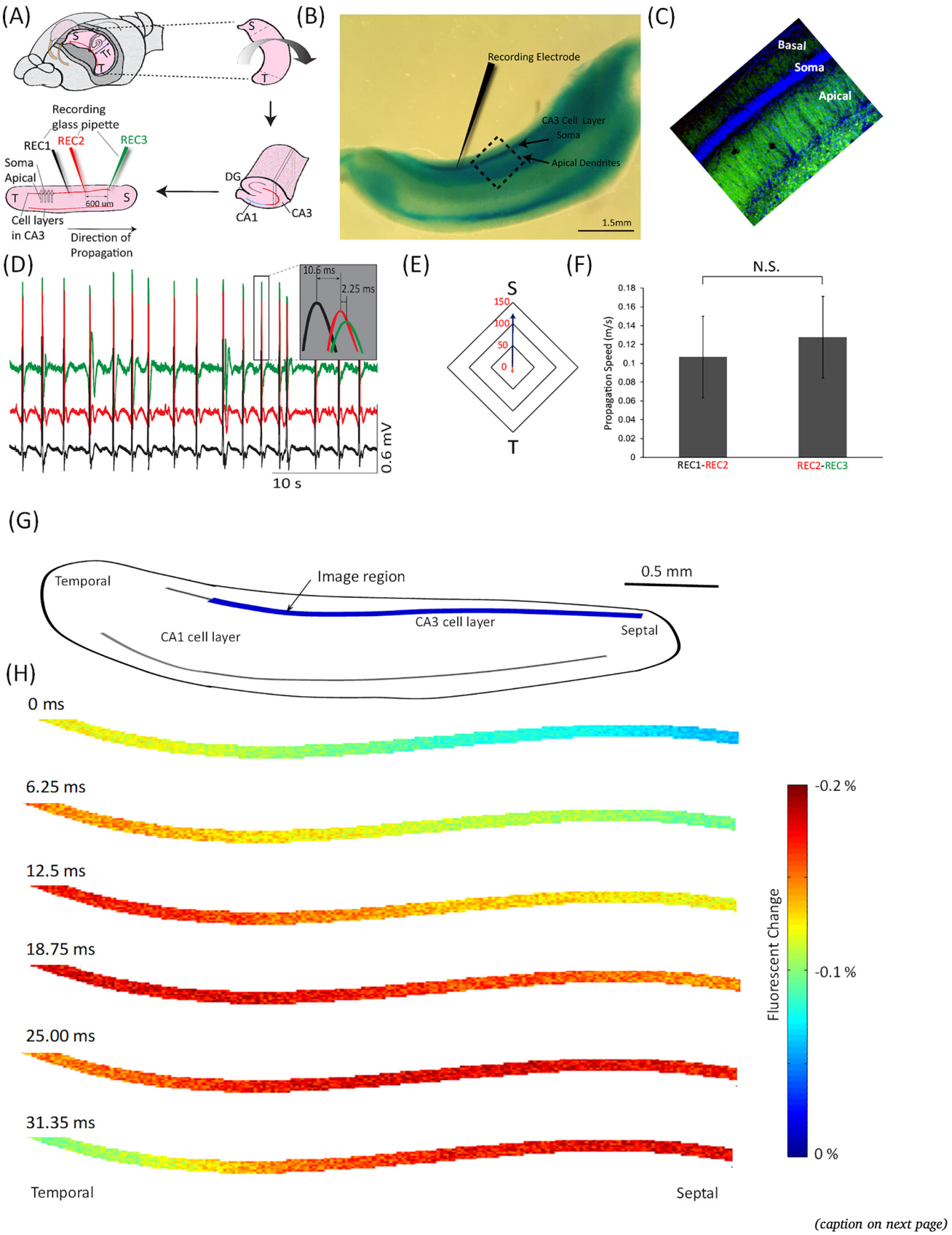


*(caption on next page)*

testing shows the field clamp system can cancel the measured voltage by applying appropriate current. A pair of extracellular recording electrodes were placed in the tissue to record the transverse electric field (direction parallel to the dendritic tree axis). Please see the supplemental document describing the derivation of the extracellular electric field clamp.

**Fig. 1.** Spontaneous epileptiform activity propagating in the longitudinal hippocampal slice preparation. (A) Anatomical structure of rodent hippocampus. A single hippocampus is extracted and oriented for slicing along the longitudinal axis. Slices are cut at 400 μm thickness. Please refer to the previous publication for more details. (B) Sample longitudinal hippocampal slice stained for cresyl violet blue that shows the pyramidal cell layers as dark blue lines CA3 cell layers observed along with positioning of recording electrodes. (C) Insert: confocal imaging showing overall architecture of the longitudinal slice. Dark blue stain is the somatic layer while green stain are the dendritic branches. (D) 4-AP initiated spontaneous activity from CA3 cell layer. REC1 (black) leads REC2 (red), which leads REC3 (green) in the direction of propagation. (E) Analysis of propagation direction. Each box represents the number of events. The size of the arrow indicates how many events propagate with respect to direction (T to S, or S to T). 125 out of 135 events propagate from temporal to septal (blue arrow) region of the hippocampus ($n = 6$ slices). (F) Analysis of propagation speed shows that there is no significant difference between REC1-REC2 (0.10 ± 0.04 m/s) and REC2-REC3 (0.13 ± 0.05 m/s) (80 spikes, 4 slices). (G) Setup for optical imaging region of interested using VSFP-Butterfly 1.2 transgenic mice. (H) An example of a 4-AP induced wave from voltage imagining showing that a spike propagated from the temporal site to septal site in the hippocampus. (For interpretation of the references to colour in this figure legend, the reader is referred to the web version of this article.)

### 2.6. Isopotential experiment setup

Two recording electrodes (REC1 and REC2) were positioned along the cell layer of the hippocampal slice. An isopotential barrier/electrode was constructed from a single column of four 30 μm diameter tungsten electrodes that were positioned between the recording electrodes in the cell layer (Fig. 4A). This array of electrodes covered the soma and dendritic trees, which were then grounded in the bath.

### 2.7. Data and statistical analysis

Data collected from these studies were processed in MATLAB for peak analysis and time-delay calculations (cross-correlation). During extracellular electric field clamp study, stimulus artifacts from the recording channels were removed by subtracting the feedback stimulation signal. A paired *t*-test statistical analysis was done under the two different conditions: propagation speed and amplitude. A statistical significance criterion of $\alpha = 0.05$ was used for all tests. Results are shown as mean ± standard deviation of the mean.

## 3. Results

### 3.1. 4-AP induced activity propagates along the longitudinal direction of the hippocampus

We studied the propagation of spontaneous epileptiform activity induced by 4-AP in rodent hippocampal slices in the longitudinal direction as the cells are tightly packed and arranged with soma and basal/apical dendrites parallel to adjacent cells (Fig. 1B,C). Spontaneous activity was observed in the presence of 4-AP, an epileptogenic compound that makes neurons hyper-excitable by blocking voltage-gated potassium channel ($I_A$), as well as in a non-synaptic environment with low calcium aCSF (Lian et al., 2001; Louvel et al., 1994) (Fig. 1D). To confirm that the activity observed was indeed propagating, direction and speed or the spontaneous waves were calculated. Propagation direction was determined from the sign of the time delay between recording electrodes. It was noted that activity propagated mostly from the temporal site to the septal site of the tissue (Fig. 1E, 125 of 135 events, 6 slices). Propagation speeds were estimated in the temporal and septal sides of the slice by measuring between REC1-REC2 (0.10 ± 0.04 m/s) and REC2-REC3 (0.13 ± 0.05 m/s) respectively, with an overall mean speed of 0.12 ± 0.06 m/s. There was no significant difference between the two speeds (Fig. 1F, 156 spikes, 6 slices) suggesting that the propagation speed is uniform. In addition, electrophysiology recording results were supported by optical recordings. Spontaneous activity images were captured in longitudinal hippocampal slices from transgenic mice that express the voltage sensitive fluorescent protein (VFSP-Butterfly 1.2) in the neuronal cytoplasm transgenic mice (Akemann et al., 2012). These mice use calcium/calmodulin-dependent protein kinase II alpha (Camk2a) promoter to direct the expression of VSFP to pyramidal neurons by a Cre-mediated recombination system. The imaging field of view was on the hippocampal cell layer to capture the propagating wave while obtaining the largest region of observation (Fig. 1G). Fig. 1H shows sample image frames of the spontaneous epileptiform wave propagating through the hippocampus (0.12 ± 0.01 m/s, 60 events, 6 slices). Previous experiments and computer stimulation have suggested that events propagating at that speed do not require synaptic transmission (Zhang et al., 2014; Qiu et al., 2015).

### 3.2. Spontaneous epileptiform activity propagates non-synaptically through a cut

To test the hypothesis that 4-AP induced epileptiform activity truly propagates non-synaptically in the hippocampus, a physical cut was made *in vitro*, severing all mechanisms that require physical neuron to neuron communication. Extracellular recording electrodes were placed in the septal and temporal regions to track the electrical activity (see Fig. 2A). 4-AP induced waves were observed to propagate from REC1 to REC2 at a speed of approximately 0.1 ± 0.01 m/s (Fig. 2A, $n = 92$ spikes, 6 slices). Once a baseline activity had been established, a cut was made across the entire hippocampal slice using a scalpel blade. To ensure that the cut was complete, the cut ends were separated and rejoined. It was found that separating the tissue > 400 μm resulted in activity still being initiated on one half of the slice with no activity observed on the other side of the cut (Fig. 2B, $n = 60$ spikes, 6 slices). Activity was recorded once the two sides were put back together and spontaneous activity was observed on the other side of the cut propagating in the same direction. The wave appears to propagate through the cut with a speed of 0.09 ± 0.01 m/s, similar to that observed without the cut (Fig. 2C, $n = 104$ spikes, 6 slices). We then separated the tissue to test the robustness of the propagation by measuring activity as we increased distance between each half of the slice. Using a paired *t*-test, no significant difference in propagation speed was found before and after a cut has been made (Fig. 2D). These results show that activity arriving at the proximal cut end can recruit neurons on the distal end of the cut.

We then measured the electric field amplitudes capable of inducing a spontaneous propagating wave in the hippocampus. Recording electrodes were positioned along the soma and apical dendrites, and extracellular voltages were measured (Fig. 2E). Electric fields were calculated by taking the difference in voltages and dividing by distance. Endogenous electric field amplitudes were found to be in a range from 2 to 6 mV/mm (Fig. 2F) with a mean value 3.9 ± 0.9 mV/mm ($n = 61$ events, 5 slices).

### 3.3. Canceling the endogenous electric field with an extracellular electric field clamp blocks propagation of epileptiform activity

We then hypothesized that a locally applied electrical field of equal amplitude and opposite polarity to that of an arriving wave should completely block the propagation of the wave. By clamping the extracellular field at zero, we determined whether endogenous electric fields are necessary for propagation of non-synaptic spontaneous activity. We, therefore, developed a technique to control the extracellular electric field with a clamping circuit capable of measuring the field of an arriving wave and applying current extracellularly to set it at zero (see supplemental section for detailed methodology and validation of the

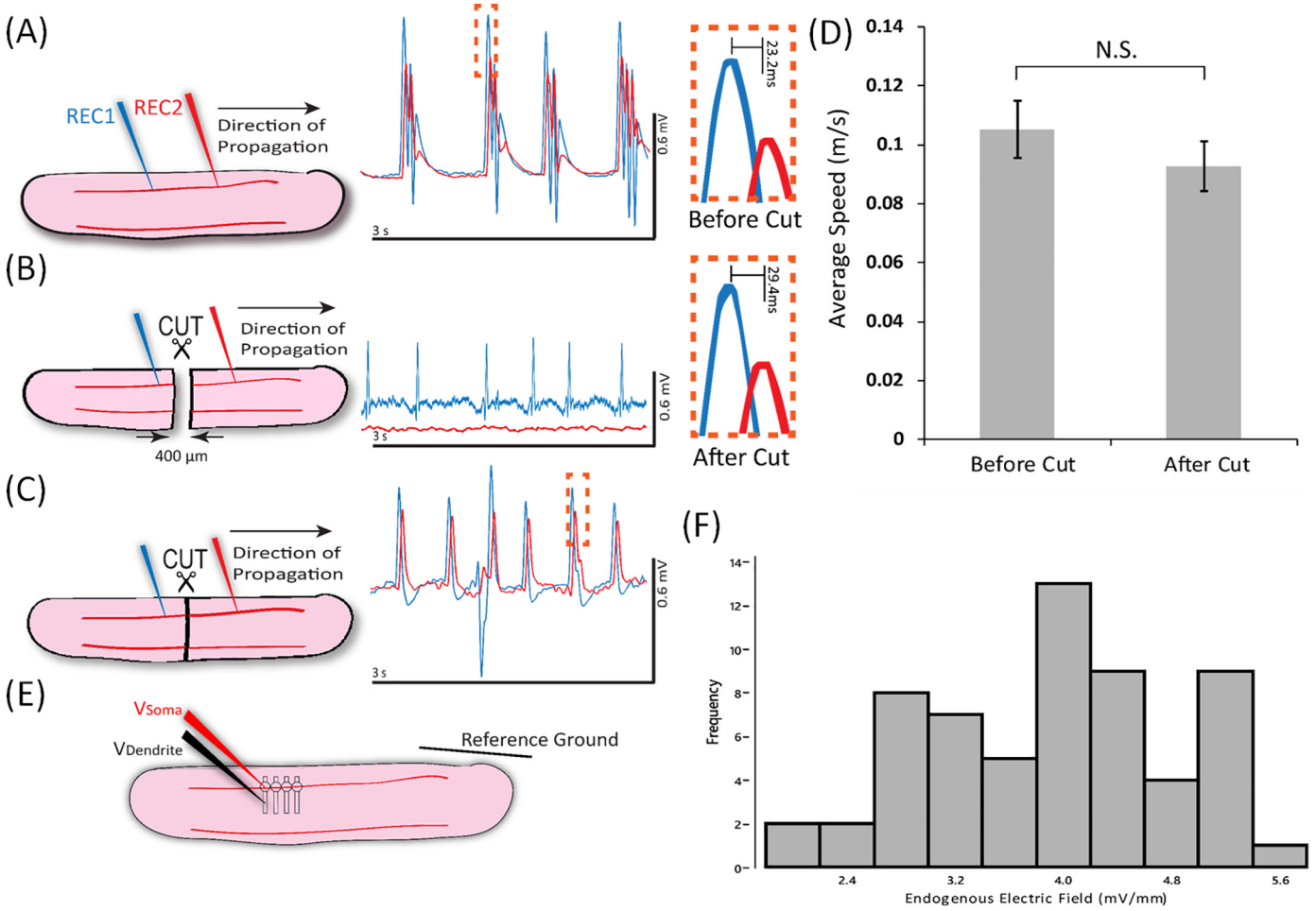


**Fig. 2.** Spontaneous propagation through a cut. (A) Baseline recording of spontaneous activity propagating from REC1 to REC2. The average delay is 23.2 msec. (B) A physical cut is made across the entire slice using a scalpel and verified by separating the two halves to ensure that all connections have been severed. The robustness of the cut was tested with one part of the slice pulled away until no synchronized activity was observed. Indicates that activity is indeed propagating through the cut. (C) Tissue halves were then put back together, and activity was observed to be propagating from REC1 to REC2. The average delay is 29.4 msec. (D) Analysis of the average speed before and after cut shows no significant difference. (E) Schematic of the instrumental system used to measure the endogenous electric field. Two recording electrodes are positioned in line with the soma and apical dendrites, and the voltages are recorded. The voltage difference is divided by the distance between the electrodes to determine the electric field. (F) Histogram of the measured endogenous electric field from 4-AP induced activity propagating in an intact longitudinal hippocampal slice (60 spikes, 4 slices).

clamping circuit, Fig. S1, S2). Extracellular electrodes were placed in the hippocampal longitudinal slice to record the transverse electric (direction parallel to the dendritic tree axis) (Fig. 3A). Spontaneous activity induced by 4-AP propagates through the cell layer as observed by the three recording electrodes (REC1 to REC3), traveling at a speed ~0.12 ± 0.03 m/s (Fig. 1D). Two extracellular stimulating electrodes were positioned outside the cell layer in the direction parallel to the longitudinal axis of the dendritic tree to generate the field. A pair of recording electrodes was position in the tissue to measure the electric field (REC2 and its reference electrode were used to measure the endogenous electric field for the clamp). A closed-loop feedback circuit was used to apply sufficient current to cancel the field in the tissue (see supplemental section for additional details). With the clamp ON, spontaneous epileptiform waves appeared to stop propagating at REC2 as indicated by the lack of activity at distal electrodes REC2 and REC3 (located on the distal side of the clamp) (Fig. 3B). Spontaneous waves were still observed at the proximal electrode REC1 with the clamp is ON. Voltages were measured at all 3 recording sites before, during, and after the clamp was applied. Spontaneous activity reappeared and continued to propagate after the clamp was removed with no change in speed from before the clamp was applied. Normalized amplitude of the recorded voltages showed that during the application of the clamp, there was a significant decrease in amplitude in both REC2 and REC3 channels (Fig. 3C, $n = 12$ slices, $t$-test, $p \leq .01$).

To further ensure that electric field coupling is a key mechanism in the propagation of spontaneous epileptiform activity, the electric field clamp was applied to the longitudinal hippocampal slice under non-synaptic conditions. Under low calcium (0.2 mM) aCSF, 4-AP induced epileptiform activity was observed to propagate in the longitudinal hippocampal slice from REC2 to REC3 (Fig. 3D**)**. Since REC1 electrode was not affected by the electric field clamp, only two recording electrodes were used to test the field clamp under non-synaptic conditions. Again, voltages were recorded before, during, and after the extracellular electric field clamp was applied. With the clamp ON, activity was observed to be blocked (Fig. 3D). When the clamp was removed, activity reappeared and continued to propagate with no change in speed from before the clamp was applied. Analysis of amplitudes when the clamp was OFF or ON showed a significant decrease with the clamp on ($n = 12$ slices, t-test, $p \leq .01$) (Fig. 3E). From these results, observing a block in propagation beyond REC2, supports the hypothesis that epileptiform activity is propagating in the hippocampus by electric field coupling alone.

Measurement of the speed of propagation in the proximal region with the clamp ON from REC1 to REC2 shows a significant decrease

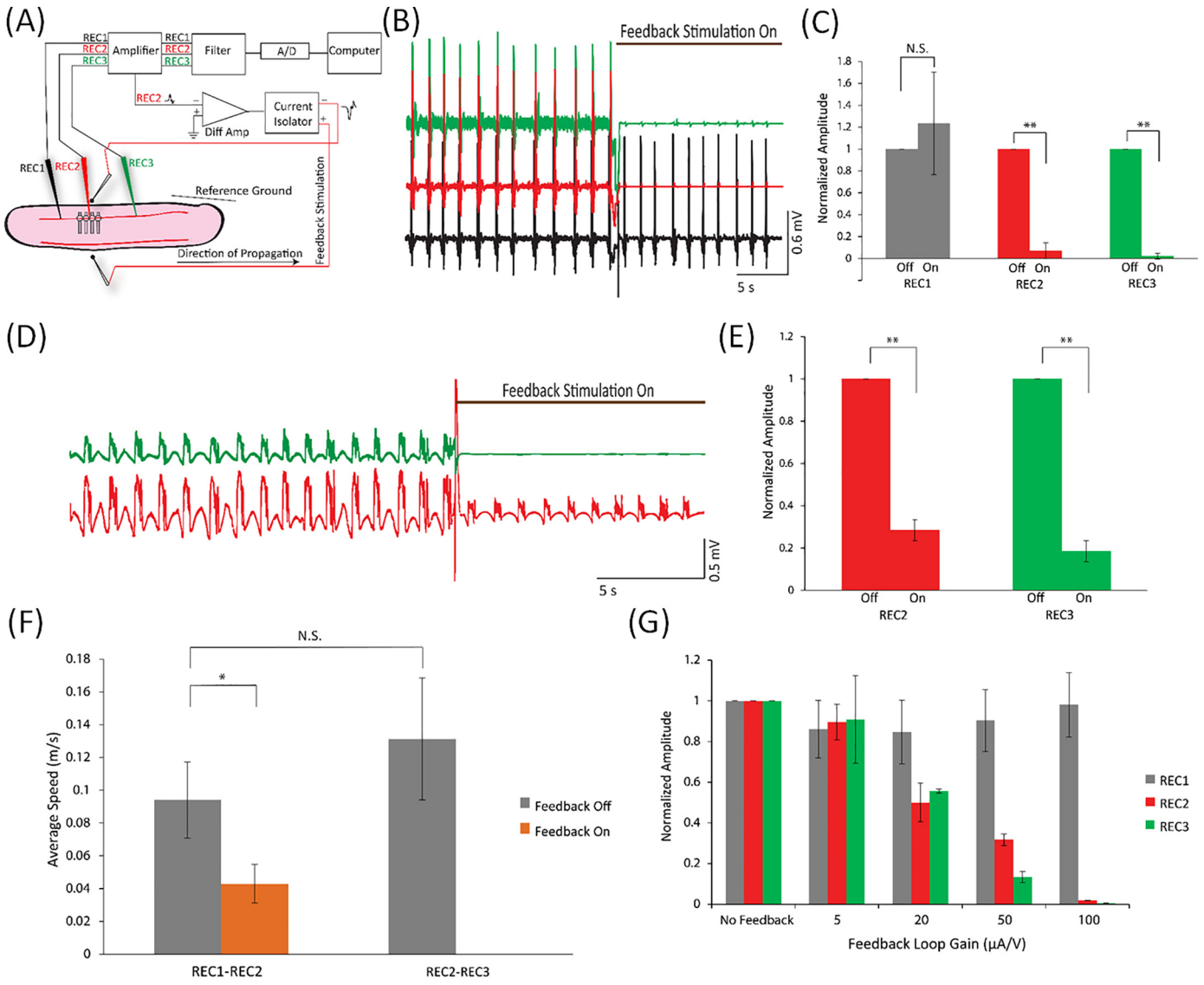


**Fig. 3.** Extracellular electric field clamp. (A) Diagram of the extracellular electric field clamp set-up. This circuit forces the extracellular electric field within the cell layer to be set equal to near zero depending on the gain of the feedback loop. Neural activity propagates from REC1 to REC3. REC2 signal is used as the feedback signal for stimulation. (B) 4-AP induced spontaneous activity propagating from REC1 to REC3. With the electric field clamp turned ON the amplitudes of the spikes in REC2 and REC3 decreased. (C) Normalized amplitude of voltages recorded at each recording site with and without electric field clamp ON. A significant decrease in amplitude observed in both REC2 and REC3 (** $p \leq .01$). (D) Extracellular electric field clamp in the presence of a pre-synaptic blocker (low calcium aCSF). Since there was no effect on REC1 with the clamp ON, only REC2 and REC3 electrode were measured for this set of experiments. 4-AP/low calcium-induced spontaneous epileptiform activity propagating from REC2 to REC3. With electric field clamp turned ON, the amplitudes of the spikes decreased in REC2 and REC3. (E) Normalized amplitude of voltages recorded at each recording site with and without electric field clamp ON. A significant decrease in amplitude observed in both REC2 and REC3 (** $p \leq .01$). (F) 4-AP initiated propagation speed decreases during stimulation ($p < .01$). (G) Effect of varying the feedback gain of electric field clamp on spontaneous activity. Normalized amplitude of propagating signal during stimulation with variable feedback. REC1 is not significantly affected by the changing feedback while REC2 and REC3 see a significant reduction in amplitude after 20 μA/V ($p < .01$).

from 0.09 ± 0.02 m/s to 0.04 ± 0.01 m/s ($p < .01$) (Fig. 3F). It is not possible to measure the speed of propagation between REC2 and REC3 as the activity does not propagate between the two electrodes when the field clamp is ON. This result indicates that the applied field slows down the incoming wave as expected from the anti-field.

The derivation of the closed-loop control system of the electric field (see Fig. S1) indicates that changing the feedback gain should affect the amplitude of the suppression. By increasing the feedback gain (5, 20, 50, 100 (μA/V), it was indeed observed that the amplitude of the propagating wave (REC2 and REC3) was significantly reduced in amplitude with a feedback gain of > 20 μA/V ($p < .01$) (Fig. 3G). However, the amplitude recorded at the proximal electrode REC1 was not significantly affected suggesting that the clamping effect is local and did not affect the location of the source of the incoming wave.

### 3.4. Increasing the conductivity along the cell layer decreases the magnitude and propagation speed of epileptiform activity

Another way to cancel the electric fields generated by neural activity is to decrease the resistivity of the solution locally. We hypothesized that if the spontaneous activity is indeed propagating by electric fields, then increasing the conductivity within the tissue should significantly affect the amplitude of the electric field on the distal side. Two recording electrodes (REC1 and REC2) were positioned along the cell layer of the hippocampal slice. A high conductivity array was constructed from a single column of four 30 μm diameter tungsten

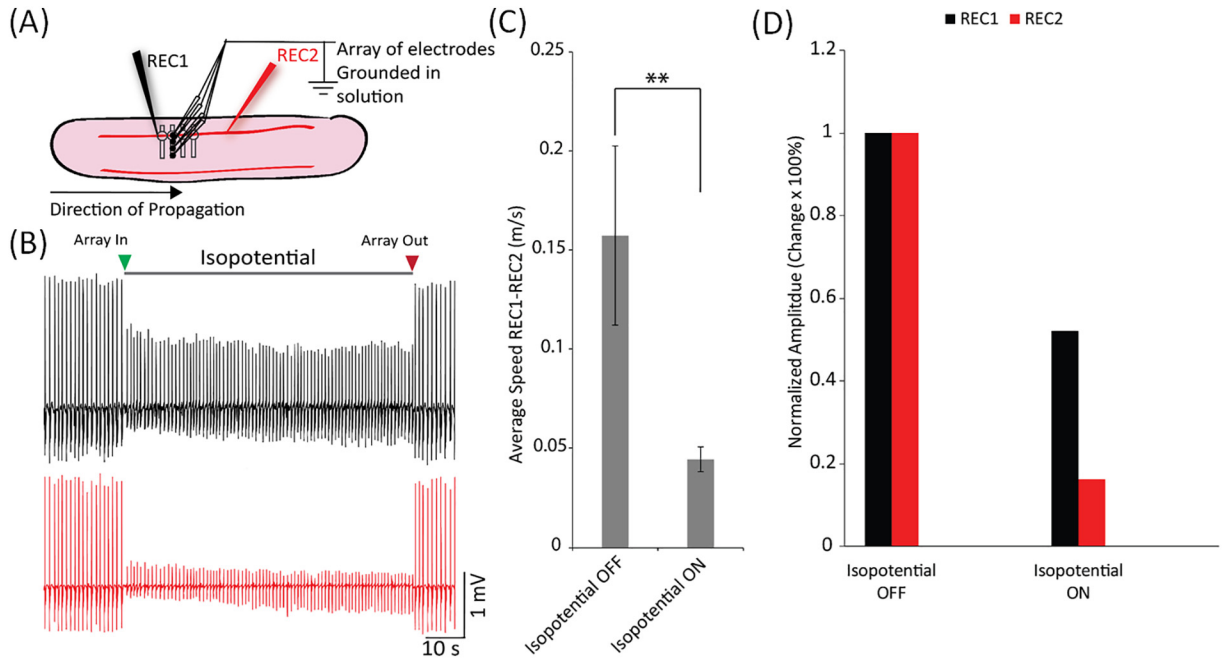


**Fig. 4.** High conductance arrays decrease speed of propagation. (A) Schematic of the experimental setup: an array of tungsten microelectrodes is placed within the tissue to create an equipotential line at zero volts in a direction parallel to the axis of the dendritic tree. (B) Example recording with array inserted (green arrow) and then removed after some time (red arrow). A decrease in amplitude is observed during isopotential application. (C) The average speed of activity decreased significantly when array applied (**$p \leq .01$). (D) Measured a significant decrease in amplitude when the array is applied (REC1: 48% decrease, REC2: 84% decrease). (For interpretation of the references to colour in this figure legend, the reader is referred to the web version of this article.)

electrodes positioned between the recording electrodes in the cell layer (Fig. 4A). This array of electrodes penetrated the soma and dendritic trees, which were then grounded in the bath. With the high conductivity region applied, the magnitude of propagating activity decreased at both recording sites (Fig. 4B). Propagation speed before the application of the high conductivity array was measured to be 0.16 ± 0.05 m/s ($n$ = 130 spikes, 4 slices), but significantly decreased to approximately 0.04 ± 0.01 m/s (Fig. 4C, $p < .01$, $n$ = 100 spikes, 4 slices). Analysis of the amplitude showed a significant decrease in amplitude in both recording channels when the isopotential array was inserted (Fig. 4D, $p < .05$). With the high conductivity array inserted, amplitudes recorded by REC1-2 decreased by 48% and 84% respectively. These results indicate that a high conductivity in the extracellular space did not block the propagation, but can affect both the propagation speed and the amplitude of the propagating event.

### 3.5. *Applied electric fields can trigger self-propagating waves in the longitudinal hippocampal slice*

The experiments reported above indicate that the wave is self-propagating whereby depolarized neurons generate an extracellular electric field that recruits neighboring cells. To test this hypothesis, we then applied electric stimulation to the tissue with current producing electric fields amplitude similar to amplitudes observed during spontaneous propagation. Under a lower concentration of 4-AP aCSF (50 μM), two recording electrodes were positioned in the cell layer of the slice (REC1 and REC2). A pair of stimulating electrodes spaced approximately 1 mm apart was positioned on the temporal side of the hippocampus slice in line with the soma and apical dendrites (Fig. 5A). An electric field pulse of 2–7 mV/mm (0.5–2 mA stimulation, 100–200 msec pulse width) was generated to initiate activity in the hippocampus (Ghai et al., 2000) with a duration similar to the spontaneous events. Electric fields were measured at the stimulation site as well as in the tissue during stimulation. An example of a 5 mV/mm field pulse generating a propagating wave is shown in Fig. 5B. We then measured the endogenous electric field during a wave propagating through the hippocampus. These values are within the same range to the endogenous field we measured as well as what has been reported in literature (Radman et al., 2007; Ghai et al., 2000; Weiss and Faber, 2010) It was observed that the field generated by initiated activity (5.13 ± 0.88 mV/mm) was not significantly different to 4-AP spontaneous activity (4.99 ± 1.14 mV/mm), which was observed after increasing the concentration of 4-AP (100 μM) concentration in the same slice (Fig. 5C, 60 spikes, 5 slices). These waves initiated by an electric field propagated from REC1 to REC2 with an average delay of 11 ± 3 msec (corresponding to a propagating speed of 0.09 ± 0.03 m/s, 50 spikes, 4 slices). When compared to spontaneous 4-AP activity, the delay was not significantly different (Fig. 5D). Taken together, these results support the hypothesis that the 4-AP induced waves are self-propagating by electric field coupling.

## 4. Discussion

This study focuses on the characterization of a new mechanism of propagation of neural activity in the brain. The average propagating speed of epileptiform events observed in this study is about (0.1 m/s), and the results of this experiments indicate that endogenous electric fields play an essential role in the propagation of events at that speed. Although electric fields with low amplitudes (1 to 5 mV/mm) are known to be able to modulate neural membrane potentials (Anastassiou et al., 2010), they are not thought to be strong enough to activate neurons. In more excitable tissue such as in the presence of 4-AP, these electric fields should be able to not only modulate, but also excite neural propagation.

Assuming that the 4-AP induced waves are self-propagating by electric field coupling, then they should be able to proceed through a complete cut of the tissue since that would show that 1) the wave generates an electric field capable of activating the cells on the other side of the cut and 2) the mechanism must be electric field coupling since other forms of propagation except for diffusion have been eliminated. Although diffusion can propagate through a cut, the speed of propagation through the cut is not compatible with this mechanism

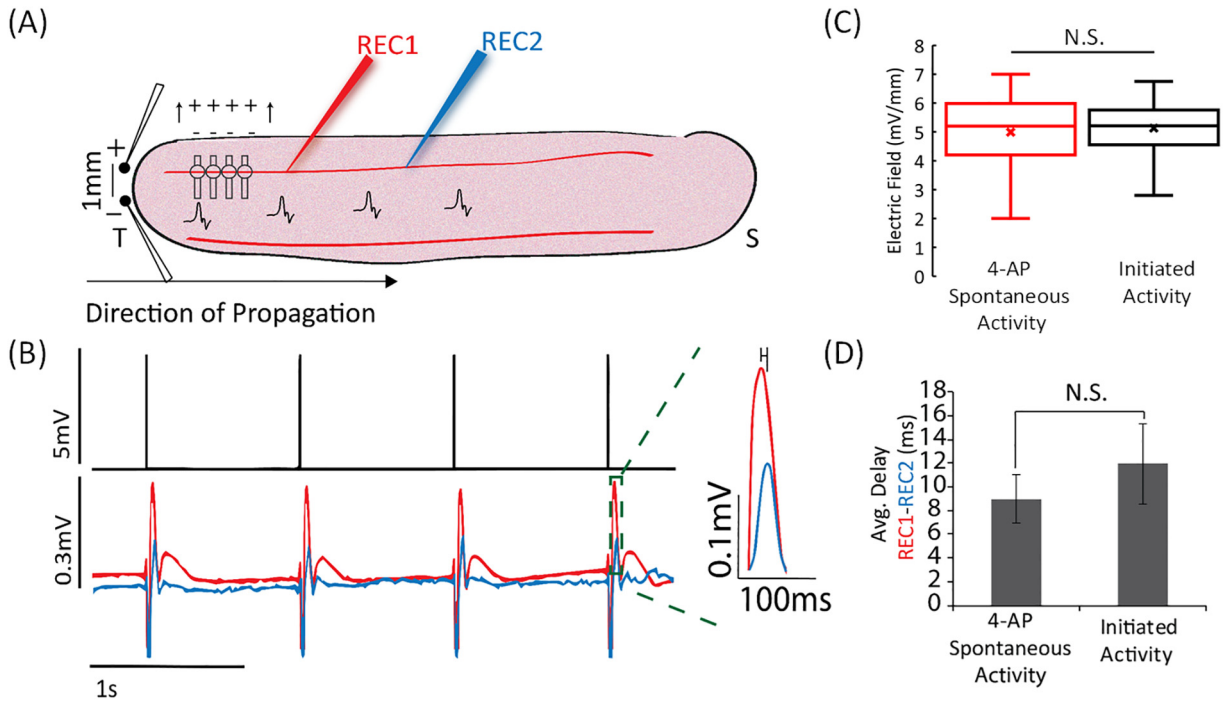


**Fig. 5.** Applying an electric field of similar endogenous amplitudes induces a propagating neural wave. (A) Schematic of the experimental setup: Electric field generated on the temporal side of the tissue with two stimulating electrodes placed 1 mm apart. (B) Stimulation with an electric field set at 5 mV/mm induces a propagating wave observed going from REC1 to REC2. (C) Measured endogenous electric fields generated by a stimulating field is not significantly difference when compared to electric fields from 4-AP induced activity. (D) Analysis of the wave propagating shows no significant difference in delay (conduction velocity) between REC1 and REC2 under both spontaneous activity and initiated activity.

(Durand et al., 2010b). The experiments reported above do show that propagation goes through a cut, strongly suggesting that the mechanism of propagation involves ephaptic or electrical field coupling. Furthermore, this endogenous field coupling mechanism makes strong predictions about the interaction between endogenous fields and neural tissue.

One prediction is that the amplitude of the electric fields involved in the propagation must fall within a range capable of modulating neural activity. It has been reported that extracellular electric fields can alter the activity of single neurons and/or network. Experiments have shown that uniform DC electric fields applied to neural tissue can modulate neural activity by hyperpolarizing or depolarizing cells (Bikson et al., 2004; Lian et al., 2003). Electric field coupling has also been shown to synchronize axons and allow for specific action potential timing (Bokil et al., in press; Radman et al., 2007; Richardson et al., 2003). Endogenous electric fields are known to induce extracellular voltage changes of < 0.5 mV and fields under 5 mV/mm (Weiss and Faber, 2010). In the present study, we provide experimental evidence indicating that spontaneous epileptiform activity induced by 4-AP propagating in the hippocampus generate electric field amplitudes in the range of 2–6 mV/mm. These fields amplitudes are similar to those known to generate electrical field effect in the hippocampal slices, approximately 5 mV/mm (Radman et al., 2007; Ghai et al., 2000), and in the cortex, approximately 4.5 mV/mm (Fröhlich and McCormick, 2010). The data presented in this study suggests that the amplitudes of the endogenous electric fields are sufficient to not only modulate neural activity in hippocampal neurons, but also recruit neurons across a small gap to generate a wave.

Another prediction is that a wave propagating by electric field coupling requires that an applied electric field in its path should affect the speed and amplitude of propagation. Canceling the extracellular electric field created by an incoming event should block propagation. This experiment requires a way to record the electrical field and control it. To achieve this goal, we modified the concept of intracellular voltage clamp (Hodgkin et al., 1952) to build an extracellular electrical field clamp. This novel concept was tested and validated by showing that an electrical field can be clamped to zero in a specific location (see Fig. S2 for validation). When applied to the propagating waves, the clamp completely blocked the transmission of the events by canceling the incoming field. Another possible mechanism for the effect is that the applied currents generated by the electric field clamp produce membrane hyperpolarization. However, based on the polarity of the applied current during the clamp, the source of the spike generation in the dendrites is depolarized not hyperpolarized.

Another method to decrease the effect of the electric field without affecting membrane polarization is to decrease the conductivity of the extracellular space. Results from experiments with a high conductivity array confirm the existence of an endogenous field as observed by a decrease in amplitude and propagation speed. The decrease of the amplitude and speed cannot be explained by damage to the tissue generated by the insertion of a high number of electrodes in the array since activity amplitude and speed returned to baseline levels following removal of the short-circuit electrode array. The fact that these experiments did not completely eliminate the propagation can be explained by the following two facts: 1) the spatial extent of the field is much larger than the electrode array and 2) the electrode array cannot generate a true short circuit between the neural sinks and sources in the tissue producing the electrical field since the interface between the metal and ionic solution is best modeled as a capacitor. Therefore, the net effect of the electrode array is to increase the bulk conductivity of the volume conductor thereby decreasing the amplitude of the fields.

A self-propagating wave was supported by two separate experiments. 1: Neurons located on the proximal side of a cut tissue were able to recruit neurons on the distal side (Fig. 2). 2: In a separate experiment, stimulating temporal region of the intact hippocampus with known endogenous field strength (2–7 mV/mm) generated a self-propagating wave through the intact slice (Fig. 5). Applied stimulation could generate waves propagating at the same speed and amplitude as

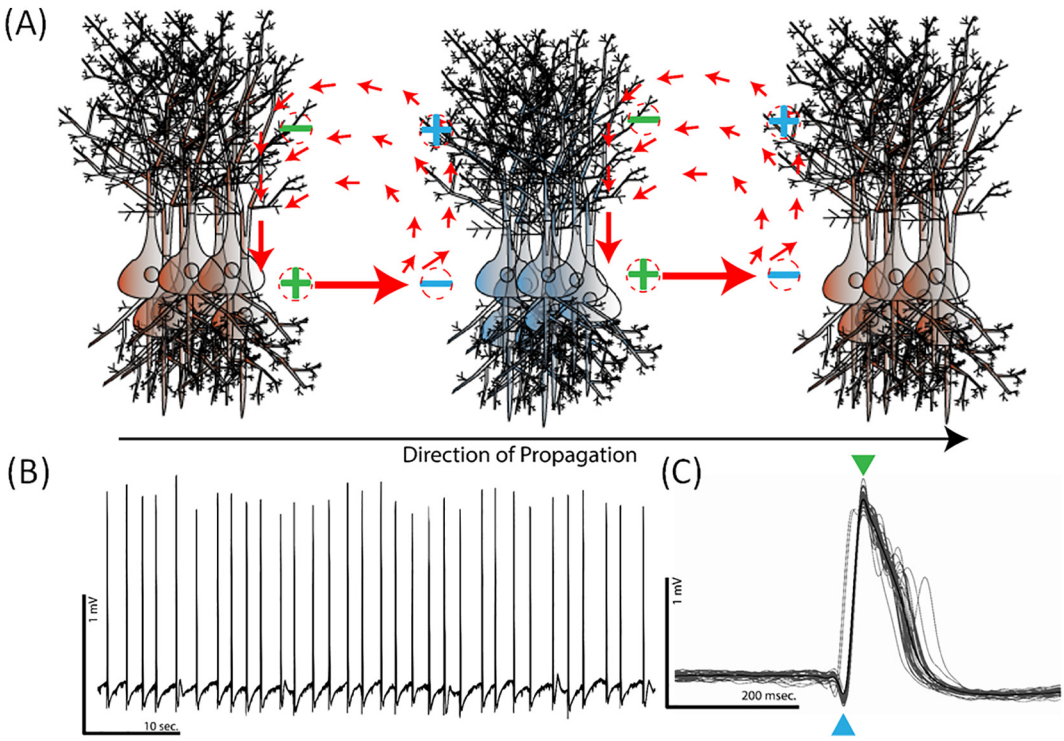


**Fig. 6.** (A) Electric coupling mechanism. A group of pyramidal cells (1st group of cells in red) become excitable and depolarize in the dendritic tree (NMDA dependent), creating a current sink in the dendrites. An electric field is generated between the soma and the dendrites in the extracellular space (green dipole). This electric field passively depolarizes the neighboring neurons (cells in blue) as indicated by the blue dipole, and the cycle repeats. (B) Sample extracellular recording of spontaneous epileptiform activity in the longitudinal hippocampal slice. (C) 4-AP wave characteristic in the soma region. The passive sink (blue arrow) proceeding the active spike depolarization (green arrow) can be observed. (For interpretation of the references to colour in this figure legend, the reader is referred to the web version of this article.)

those propagating spontaneously thereby suggesting that the hippocampus cell network is capable of mediating self-propagating waves *via* small electric fields. This phenomenon was predicted by previous computer simulations (Qiu et al., 2015) and validated experimentally in the present study.

The present study shows that the amplitudes of endogenous electric fields are high enough to generate spontaneous activity and further implies that 4-AP epileptiform can self-propagate by triggering new activity in the neighboring region through electric field coupling. Moreover, the present study shows that canceling the fields generated by the epileptiform activity can prevent the propagation and thus we can infer that these fields are required to sustain the propagation. Therefore, the experimental results in this study support the notion that epileptiform activity can propagate through the electric field coupling alone. However, the interaction between soma and dendrites to generate electric fields or the intracellular response to these fields are still not clear. Previous computational modeling suggests that NMDA receptors are involved during this process (Chiang et al., 2018).

A possible mechanism of propagation mediated by electric field coupling in the hippocampus is illustrated in Fig. 6A. In the presence of 4-AP, groups of neurons become more excitable and generate epileptiform activity (Fig. 6B). As the group of neurons depolarizes, a large sink is created in the dendrites by NMDA inward currents (Buzsáki et al., 2012). The resulting extracellular field produces an outward current in the dendrites (source) in neighbor cells as well as a passive inward current (sink). This passive sink can be observed in the somatic region of the slice preceding the wave (Fig. 6C). The passive membrane depolarization then activates inward NMDA current activating those same cells. This process repeats itself, thereby generating a self-propagating wave. This source-sink relationship between soma and dendrites has been previously investigated by others (Dickson et al., 2006; Isomura et al., 2006; Makarov et al., 2010; Makarova et al., 2010; Makarova et al., 2011; Fernández-Ruiz and Herreras, 2013), but will need to be validated experimentally in the future.

The present study shows that the neural activity can propagate by a non-synaptic mechanism of electric field coupling based on several experimental results. This non-synaptic mechanism could explain how micro-seizures could possibly recruit neurons through large areas of the brain to generate larger seizures (Stead et al., 2010). In addition, this mechanism could explain the low success rate of multiple subpial transections, a therapy by which make several cuts in the cortex to isolate the epileptogenic zone (Téllez-Zenteno et al., 2005). In principle, this treatment course prevents epileptic activity from spreading out. However, the outcome of this procedure is poor, and the long-term effects are still questionable. Only 33% of patients are seizure-free after receiving MST treatment in adults, and about 33–42% of patients are seizure free in children (Ntsambi-Eba et al., 2013; Benifla et al., 2006; Blount et al., 2004). The results of these studies could be explained by the electric field coupling phenomenon described above. It should also be noted that the non-synaptic coupling has been previously observed between hippocampal neurons but was attributed to gap junctions without clear evidence (Draguhn et al., 1998). Furthermore, we describe a novel technique (field clamp) for canceling the endogenous electric field that could be used for treating non-synaptic epilepsy in humans.

In summary, this study focused on the characterization of a new mechanism of propagation of neural activity in the brain. The results provide direct experimental evidence that 1) endogenous fields are more significant than previously thought, 2) electric field coupling can explain propagation in certain types of epileptiform activity in the brain, and 3) electric field coupling can explain the existence of self-propagating waves in the hippocampus.

## Acknowledgment

*Funding*

This work was funded by grants from the National Institute of Health (NIH/NINDS 5R01NS060757-07: Detection and Control of Epilepsy, NIH/NIBIB 5T32EB004314-19: Integrated Engineering and Rehabilitation.

*Author contributions*

R.S.S and D.M.D designed the study; R.S.S, C.-C.C., performed the experiments; L.E.G-R performed longitudinal hippocampal slice histology; R.S.S, C.-C.C, M.Z analyzed data; R.S.S and D.M.D. wrote the manuscript with input from all authors.

*Competing interests*

The authors declare that they have no competing interests.

## Appendix A. Supplementary data

Supplementary data to this article can be found online at https://doi.org/10.1016/j.expneurol.2019.02.005.

## References

Akemann, W., et al., 2012. Imaging neural circuit dynamics with a voltage-sensitive fluorescent protein. J. Neurophysiol. 108, 2323–2337.
Amaral, D.G., Witter, M.P., 1989. The three-dimensional organization of the hippocampal formation: a review of anatomical data. Neuroscience 31, 571–591.
Anastassiou, C.A., Montgomery, S.M., Barahona, M., Buzsaki, G., Koch, C., 2010. The effect of spatially inhomogeneous extracellular electric fields on neurons. J. Neurosci. 30, 1925–1936.
Anastassiou, C.A., Perin, R., Markram, H., Koch, C., 2011. Ephaptic coupling of cortical neurons. Nat. Neurosci. 14, 217–223.
Benifla, M., Otsubo, H., Ochi, A., Snead, O.C., Rutka, J.T., 2006. Multiple subpial transections in pediatric epilepsy: indications and outcomes. Childs Nerv. Syst. 22, 992–998.
Bikson, M., et al., 2004. Effects of uniform extracellular DC electric fields on excitability in rat hippocampal slices in vitro. J. Physiol. 557, 175–190.
Blount, J.P., et al., 2004. Multiple subpial transections in the treatment of pediatric epilepsy. J. Neurosurg. 100, 118–124.
Bokil, H., Laaris, N., Blinder, K., Ennis, M., Keller, A., 2019. Ephaptic interactions in the mammalian olfactory system. J. Neurosci. 21, RC173. https://doi.org/10.1523/jneurosci.21-20-j0004.2001.
Buzsáki, G., Anastassiou, C.A., Koch, C., 2012. The origin of extracellular fields and currents-EEG, ECoG, LFP and spikes. Nat. Rev. Neurosci. 13, 407–420.
Chiang, C.C., Shivacharan, R.S., Wei, X., Gonzalez-Reyes, L.E., Durand, D.M., 2019. Slow periodic activity in the longitudinal hippocampal slice can self-propagate non-synaptically by a mechanism consistent with ephaptic coupling. J. Physiol. https://doi.org/10.1113/JP276904.
Chiang, C.C., et al., 2018. Slow moving neural source in the epileptic hippocampus can mimic progression of human seizures. Sci. Rep. 8. https://doi.org/10.1038/s41598-018-19925-7.
Dickson, C.T., Wolansky, T., Clement, E.A., Peters, S.R., Palczak, M.A., 2006. Hippocampal slow oscillation: a novel EEG state and its coordination with ongoing neocortical activity. Artic. J. Neurosci. Off. J. Soc. Neurosci. https://doi.org/10.1523/JNEUROSCI.5594-05.2006.
Draguhn, A., Traub, R.D., Schmitz, D., Jefferys, J.G.R., 1998. Electrical coupling underlies high-frequency oscillations in the hippocampus in vitro. Nature 394, 189–192.
Dudek, F.E., Yasumura, T., Rash, J.E., 1998. "Non-synaptic" mechanisms in seizures and epileptogenesis. Cell Biol. Int. 22, 793–805.
Durand, D.M., Park, E., Jensen, A.L., 2010a. Potassium Diffusive Coupling in Neural Networks. pp. 2347–2362.
Durand, D.M., Park, E.-H., Jensen, A.L., 2010b. Potassium diffusive coupling in neural networks. Philos. Trans. R. Soc. Lond. Ser. B Biol. Sci. 365, 2347–2362.
Fernández-Ruiz, A., Herreras, O., 2013. Identifying the synaptic origin of ongoing neuronal oscillations through spatial discrimination of electric fields. Front. Comput. Neurosci. 7, 5.
Francis, J.T., Gluckman, B.J., Schiff, S.J., Physics, D., 2003. Sensitivity of Neurons to Weak Electric Fields. vol. 23. pp. 7255–7261.
Fröhlich, F., McCormick, D.A., 2010. Endogenous electric fields may guide neocortical network activity. Neuron 67, 129–143.
Ghai, R.S., et al., 2000. Effects of Applied Electric Fields on Low-Calcium Epileptiform Activity in the CA1 Region of Rat Hippocampal Slices. pp. 274–280.
Gloveli, T., et al., 2005. Orthogonal arrangement of rhythm-generating microcircuits in the hippocampus. Proc. Natl. Acad. Sci. U. S. A. 102, 13295–13300.
Haas, H.L., Jefferys, J.G., 1984. Low-calcium field burst discharges of CA1 pyramidal neurones in rat hippocampal slices. J. Physiol. 354, 185–201.
Hodgkin, A.L., Huxley, A.F., Katz, B., 1952. Measurement of current-voltage relations in the membrane of the giant axon of Loligo. J. Physiol. 116, 424–448.
Ishizuka, N., Weber, J., Amaral, D.G., 1990. Organization of intrahippocampal projections originating from CA3 pyramidal cells in the rat. J. Comp. Neurol. 295, 580–623.
Isomura, Y., et al., 2006. Integration and segregation of activity in entorhinal-hippocampal subregions by neocortical slow oscillations. Neuron 52, 871–882.
Jeffery, K.J., Anderson, M.I., Hayman, R., Chakraborty, S., 2004. Studies of the Hippocampal Cognitive Map in Rats and Humans. *Stud. hippocampal Cogn. map rats humans*. pp. 17–39.
Jefferys, J.G., 1981. Influence of electric fields on the excitability of granule cells in guinea-pig hippocampal slices. J. Physiol. 319, 143–152.
Jensen, A.L., 2008. Thesis. Case Western Reserve University.
Kibler, A.B., Durand, D.M., 2011. Orthogonal wave propagation of epileptiform activity in the planar mouse hippocampus in vitro. Epilepsia 52, 1590–1600.
Lian, J., Bikson, M., Shuai, J., Durand, D.M., 2001. Propagation of non-synaptic epileptiform activity across a lesion in rat hippocampal slices. J. Physiol. 537, 191–199.
Lian, J., Bikson, M., Sciortino, C., Stacey, W.C., Durand, D.M., 2003. Local suppression of epileptiform activity by electrical stimulation in rat hippocampus in vitro. J. Physiol. 547, 427–434.
Liu, J.-S., et al., 2013. Spatiotemporal dynamics of high-K+-induced epileptiform discharges in hippocampal slice and the effects of valproate. Neurosci. Bull. 29, 28–36.
Louvel, J., Avoli, M., Kurcewicz, I., Pumain, R., 1994. Extracellular free potassium during synchronous activity induced by 4-aminopyridine in the juvenile rat hippocampus. Neurosci. Lett. 167, 97–100.
Maguire, E.A., et al., 2000. Navigation-related structural change in the hippocampi of taxi drivers. Proc. Natl. Acad. Sci. 97, 4398–4403.
Makarov, V.A., Makarova, J., Herreras, O., 2010. Disentanglement of local field potential sources by independent component analysis. J. Comput. Neurosci. 29, 445–457.
Makarova, J., Makarov, V.A., Herreras, O., 2010. Generation of sustained field potentials by gradients of polarization within single neurons: a macroscopic model of spreading depression. J. Neurophysiol. 103, 2446–2457.
Makarova, J., Ibarz, J.M., Makarov, V.A., Benito, N., Herreras, O., 2011. Parallel readout of pathway-specific inputs to laminated brain structures. Front. Syst. Neurosci. 5, 77.
Meeks, J.P., Mennerick, S., 2007. Action potential initiation and propagation in CA3 pyramidal axons. J. Neurophysiol. 97, 3460–3472.
Miles, R., Traub, R.D., Wong, R.K., 1988. Spread of synchronous firing in longitudinal slices from the CA3 region of the hippocampus. J. Neurophysiol. 60, 1481–1496.
Morris, R.G.M., Garrud, P., Rawlins, J.N.P., O'Keefe, J., 1982. Place navigation impaired in rats with hippocampal lesions. Nature 297, 681–683.
Ntsambi-Eba, G., Vaz, G., Docquier, M.A., Van Rijckevorsel, K., Raftopoulos, C., 2013. Patients with refractory epilepsy treated using a modified multiple subpial transection technique. Neurosurgery 72, 890–897.
Qiu, C., Shivacharan, R.S., Zhang, M., Durand, D.M., 2015. Can neural activity propagate by endogenous electrical field? J. Neurosci. 35, 15800–15811.
Quilichini, P.P., Diabira, D., Chiron, C., Ben-Ari, Y., Gozlan, H., 2002. Persistent epileptiform activity induced by low Mg2+ in intact immature brain structures. Eur. J. Neurosci. 16, 850–860.
Radman, T., Su, Y., An, J.H., Parra, L.C., Bikson, M., 2007. Spike Timing Amplifies the Effect of Electric Fields on Neurons : Implications for Endogenous Field Effects. vol. 27. pp. 3030–3036.
Richardson, K.A., et al., 2003. In vivo modulation of hippocampal epileptiform activity with radial electric fields. Epilepsia 44, 768–777.
Sanchez-Vives, M.V., McCormick, D.A., 2000. Cellular and network mechanisms of rhythmic recurrent activity in neocortex. Nat. Neurosci. 3, 1027–1034.
Schevon, C.A., et al., 2012. Evidence of an inhibitory restraint of seizure activity in humans. Nat. Commun. 3, 1060.
Stead, M., et al., 2010. Microseizures and the spatiotemporal scales of human partial epilepsy. Brain 133, 2789–2797.
Téllez-Zenteno, J.F., Dhar, R., Wiebe, S., 2005. Long-term seizure outcomes following epilepsy surgery: a systematic review and meta-analysis. Brain 128, 1188–1198.
Terzuolo, T.H., Bullock, C.A., 1956. Measurement of imposed voltage gradient adequate to modulate neuronal firing. Proc. Natl. Acad. Sci. U. S. A. 42, 687–694.
Weiss, S.A., Faber, D.S., 2010. Field effects in the CNS play functional roles. Front. Neural Circ. 4, 15.
Weissinger, F., Buchheim, K., Siegmund, H., Heinemann, U., Meierkord, H., 2000. Onsets, Spread Patterns, and Propagation Velocities in Hippocampal – Entorhinal Cortex Slices of Juvenile Rats. vol. 298. pp. 286–298.
Yang, S., et al., 2014. Interlamellar CA1 network in the hippocampus. Proc. Natl. Acad. Sci. U. S. A. 111, 12919–12924.
Zhang, M., et al., 2014. Propagation of epileptiform activity can be independent of synaptic transmission, gap junctions, or diffusion and is consistent with electrical field transmission. J. Neurosci. 34, 1409–1419.